Contract No:

This document was prepared in conjunction with work accomplished under Contract No. DE-AC09-08SR22470 with the U.S. Department of Energy (DOE) Office of Environmental Management (EM).

Disclaimer:

SRNL-STI-2017-00224

Proceedings of the ASME 2017 Pressure Vessels and Piping Conference
PVP2017
July 16-20, 2017, Waikoloa, Hawaii, United States

PVP2017-66055

BOUNDING SURFACE FLAW CONFIGURATION SUSCEPTIBLE TO STRESS CORROSION CRACKING UNDER WELDING RESIDUAL STRESS IN A MULTIPLE-PURPOSE CANISTER

Poh-Sang Lam
Materials Science and Technology
Savannah River National Laboratory
Aiken, SC 29808, USA
ps.lam@srnl.doe.gov

Robert L. Sindelar
Materials Science and Technology
Savannah River National Laboratory
Aiken, SC 29808, USA
robert.sindelar@srnl.doe.gov

Andrew J. Duncan
Materials Science and Technology
Savannah River National Laboratory
Aiken, SC 29808, USA
andrew.duncan@srnl.doe.gov

Joe T. Carter
Nuclear Programs
Savannah River National Laboratory
Aiken, SC 29808, USA
joe.carter@srs.gov

ABSTRACT

The part-through-wall crack perpendicular to the circumferential weld on the outside surface of a spent nuclear fuel (SNF) multiple-purpose canister (MPC) can be shown to be the most limiting fracture configuration driven by the welding residual stress (WRS). A series of semi-elliptical cracks of various sizes is chosen to calculate the stress intensity factors (K) under a bounding residual stress (i.e., the stress distribution that bounds all WRS in a canister). The threshold stress intensity factor (K_{ISCC}) of the canister material in the storage environment is used to determine a critical flaw size, below which the stress corrosion cracking would be unlikely to take place. This result can be considered as the flaw disposition criterion should a surface flaw be detected during the inservice inspection as required by the aging management program (AMP), and can be proposed to American Society of Mechanical Engineers (ASME) Section XI Code Case N-860, "Examination Requirements and Acceptance Standards for Spent Nuclear Fuel Storage and Transportation Containment Systems."

INTRODUCTION

Upon being discharged from the nuclear reactors, the SNF are immediately placed in wet storage pools. After sufficient time to allow for cooling through radioactive decay, they can be mechanically dried and transferred into MPCs to dry cask storage facilities known as Independent Spent Fuel Storage Installations (ISFSIs), many of which are located near the coastal regions where chloride-bearing salts mixed with dust may deliquesce under temperature and humidity conditions on the external surface of the canister and cause stress corrosion cracking in areas affected by WRS since canisters are not required to be stress relieved after fabrication and welding.

This chloride induced stress corrosion cracking (CISCC) could initiate a crack that may grow to approach the instability crack size and compromise the safety-credited containment boundary of the storage system. Therefore, the U.S. Nuclear Regulatory Commission (NRC) requires that an AMP be in place to demonstrate the structural integrity and confinement function of the canisters when a dry storage facility is applying for license extension. As a result, NRC has requested ASME Section XI to develop Code Case N-860, "Examination Requirements and Acceptance Standards for Spent Nuclear Fuel Storage and Transportation Containment Systems."

The acceptable part-though-wall surface crack size under the influence of WRS and external loads has been estimated and proposed to Code Case N-860 [1,2]. The current work is focused on CISCC, in particular, to establish a threshold stress intensity factor (K_{ISCC}) and the acceptable initial flaw size below which the stress corrosion cracking will not take place. The results can also be input to Code Case N-860.

CANISTER CONFIGURATIONS

As reported in previous publications [1,2], a typical dry cask storage system (DCSS), the Holtec International Storage Module (HI-STORM) [3,4], was selected for the present

investigation on the stress intensity factors (K) of an external semi-elliptical surface crack under WRS. The canister is a cylindrical shell made of austenitic stainless steel (304/304L, typically) [3]. The height of the canister is 4.8 m (15.8 ft), the outer diameter is 1.73 m (5.7 ft), and the thickness of the shell is 12.7 mm (0.5 in.).

The major welds in HI-STORM canister are schematically shown in Fig. 1. The upper and lower longitudinal (or axial) welds are offset slightly along the circumferential weld. Submerged arc welding (SAW) with full penetration double-V groove is applied. The weld metal is typically Type 308/308L stainless steel.

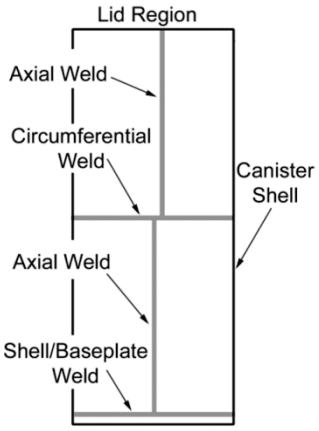

Figure 1 Holtec HI-STORM Canister Weld Schematics

WELDING RESIDUAL STRESS

Because the HI-STORM welding information is proprietary, the WRS was estimated in previous work [1] using American Petroleum Institute (API) 579 Annex E (2007 Edition) [5] by assuming an average heat input of 1080 J/mm (based on a 4 mm electrode, 889 mm/min travel speed, with 500A-32V for stainless steel with SAW process). The yield stress for WRS estimation is 274 MPa (40 ksi) that is based on API 579 recommendations [5,6] to use the base metal code minimum yield stress [7] raised by 69 MPa (10 ksi) to account for actual material property that is usually higher. Four WRS were calculated as the crack opening stresses for the surface cracks on the canister [1,2]:

1) RS1: Axial crack parallel to an axial or longitudinal weld with the residual stress perpendicular to the weld;
2) RS2: Axial crack perpendicular to a circumferential or girth weld with the residual stress parallel to the weld;
3) RS3: Circumferential crack parallel to a circumferential weld with the residual stress perpendicular to the weld;
4) RS4: Circumferential crack perpendicular to a longitudinal weld with the residual stress parallel to the weld.

These WRS distributions through the wall thickness are shown in Fig. 2 (measured from the outside diameter, OD) [1,2], from which it can be seen that the WRS components (RS2 and RS4) parallel to the welds (circumferential and longitudinal welds, respectively) are higher, as this is typically the case for the welded structures. In addition, near the canister surface, RS2 (the residual stress tends to open an axial surface crack) appears to be bounding. Therefore, this type of loading is considered in this paper. Furthermore, a bounding WRS as shown in Fig. 3 can be constructed as

$$\sigma_r = 117.435\frac{x}{t} + 411 \ \text{(in MPa)} \qquad (1)$$

where σ_r is the WRS, t is the thickness of the canister wall, and x is measured from the outside surface of the canister ($0 \le x \le t$). Note that this stress distribution is linear and is easily decomposed into a uniform membrane stress (σ_m) with a superimposed pure bending stress (σ_b). This upper bound residual stress is used for stress intensity factor calculation in this paper. The results can be used as a CISCC acceptance standard should a flaw be detected by inservice inspection. If the detected flaw is smaller than the crack size corresponding to K_{ISCC} of the material under the canister storage environment, no stress corrosion cracking should occur.

The experimental investigation of WRS in a DCSS canister was also conducted by Sandia National Laboratories [8]. This mockup canister differs slightly from the Holtec HI-STORM that is used in current analysis. The mockup canister is based on TransNuclear NUHOMS 24P design, and its dimensions are shown in Fig. 4 with a wall thickness of 15.9 mm (5/8 in.). Same as HI-STORM, the mockup canister was made of 304/304L stainless steel and the weld filler metal is 308L. The SAW process was applied to join the canister parts with multiple passes.

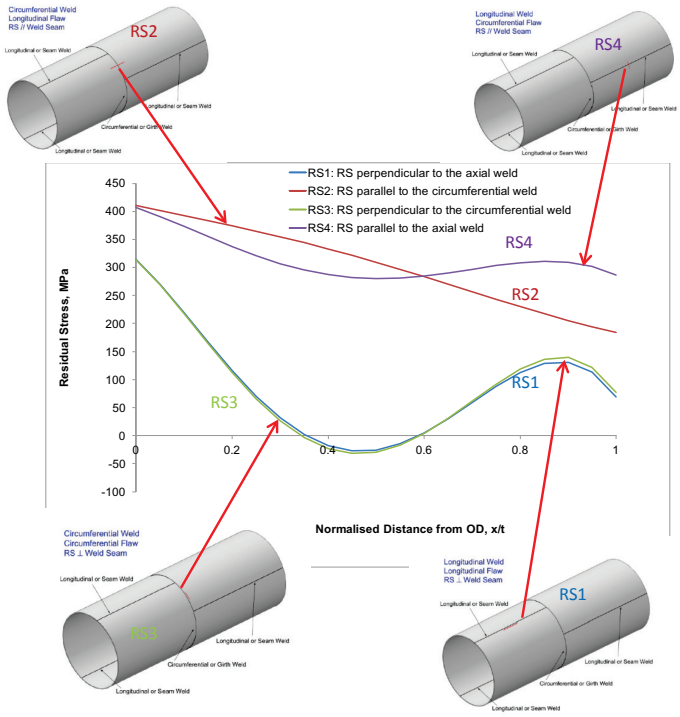

Figure 2 Residual Stress Estimated from API 579 Annex E (2007) [5] for a Holtec HI-STORM Canister

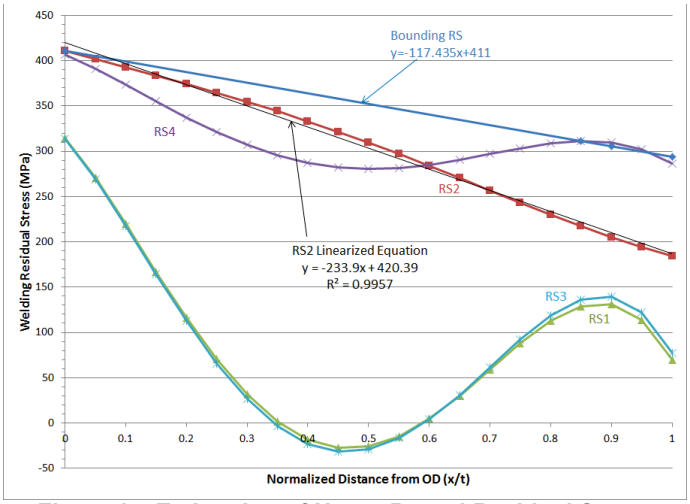

Figure 3 Estimation of Upper Bound Residual Stress

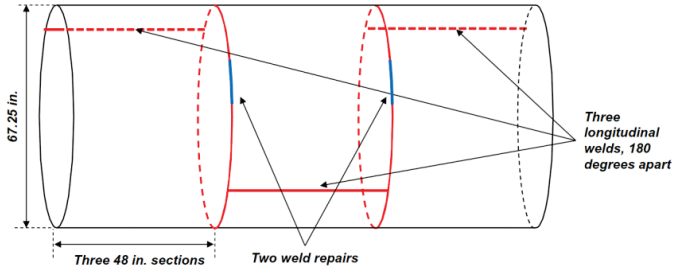

Figure 4 Sandia Mockup Canister Welds [8]
(Courtesy of Sandia National Laboratories)

Sandia National Laboratories also conducted WRS measurement by traditional Deep-Hole Drilling (DHD) and Incremental Deep-Hole Drilling (iDHD). Also conducted was the contour method which is capable of providing a stress map over the entire cross section, as shown in Figs. 5 and 6. Figure 5 represents the hoop stress in the axial cross section of the canister containing the weld, that is, the stress contour illustrates the WRS parallel to a circumferential weld (or RS2, as designated earlier). Similarly, Fig. 6 is the axial stress in a cross section containing a longitudinal weld and the stress is parallel to the weld direction (i.e., RS4)

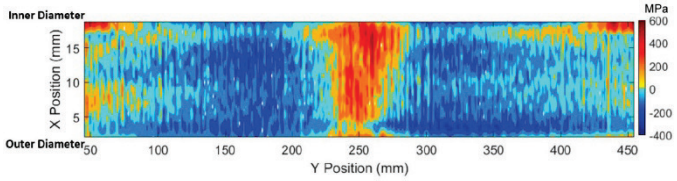

Figure 5 Residual Stress Contour Map Parallel to a Circumferential Weld through the Wall Thickness of the Sandia Mockup Canister [8] (Designated as RS2 in Fig. 2)
(Courtesy of Sandia National Laboratories)

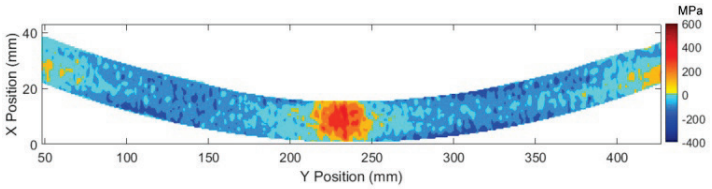

Figure 6 Residual Stress Contour Map Parallel to a Longitudinal Weld through the Wall Thickness of the Sandia Mockup Canister [8] (Designated as RS4 in Fig. 2)
(Courtesy of Sandia National Laboratories)

Although the HI-STORM and the Sandia mockup canister have different overall (but similar) dimensions and the same welding process (i.e., SAW), the actual measurement of WRS (Figs. 5 and 6) are consistent with the estimated WRS by API 579 Annex E (2007) [5] (Fig. 2). That is, Fig. 5 shows that the hoop stress in tension has a bending effect (referred to the warm colors) just as the RS2 shown in Fig. 2; while in Fig. 6, which is equivalent to RS4 in Fig. 2, the stress is more uniform and appears to be lower than that in Fig. 5. It should be mentioned that, were the WRS be estimated with the procedure in API 579 Annex 9D (2016 Edition) [6], both RS2 and RS4 would be uniform across the wall and in a much lower stress level (up to 274 MPa which is the elevated code minimum yield stress of the base metal as discussed earlier). It seems that the WRS estimation from API 579 Annex E (2007) [5] has better agreement with the Sandia measurements. Note that the WRS estimation procedure in API 579 Annex 9D (2016) [6] is based on R6 [9] and BS 7910 [10].

STRESS INTENSITY FACTORS

The stress intensity factors for cracks in a cylindrical shell can be calculated with the cumbersome procedure described in API 579 Annex C (2007) [5] or Annex 9B (2016) [6]. For simplicity, the Mode I stress intensity factor of a semi-elliptical surface crack in a flat plate solution [11,12] is used as an approximation for the current case:

$$K = (\sigma_m + H\sigma_b)\sqrt{\frac{\pi a}{Q}}F\left(\frac{a}{t},\frac{a}{c},\frac{c}{W},\varphi\right) \quad (2)$$

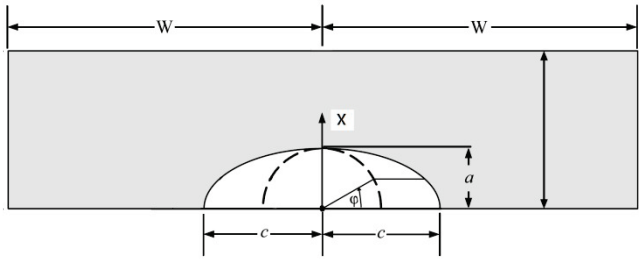

Figure 7 Definition of a Part-though-wall Surface Crack

where a is the crack depth, c is the half crack length, φ is the elliptic angle as defined in Fig. 7, t is the wall thickness, and

2W is the width of the flat plate. In the case of an axial crack in the canister, the parameter W in Eq. (2) is taken as the half height of the canister (2.4 m). The expressions for the non-dimensional functions H, Q, and F in Eq. (2) can be found in Reference [11].

The flat plate solution, Eq. (2), is shown to have sufficient accuracy in Fig. 8 for a cylindrical vessel with large radius to thickness ratio (*R/t*). In Fig. 8 the flat plate solution at the deepest point of a deep surface crack (12 mm or 94% of wall thickness) on the canister is compared with an alternative codified solution obtained with R6 procedure [2]. All the stress intensity factors are calculated with the same set of WRS (RS2) as obtained from APT 579 Annex E (2007) and are shown in Fig. 2 (Note: this is not the bounding residual stress defined by Eq. (1)). It should be mentioned that the ASME Boiler and Pressure Vessel Code, Section XI, Appendix A [12] allows the stress intensity factors for outside surface cracks to be calculated with a flat plate model because the Section XI solutions are still under development (see Articles A-3540 and A-3560).

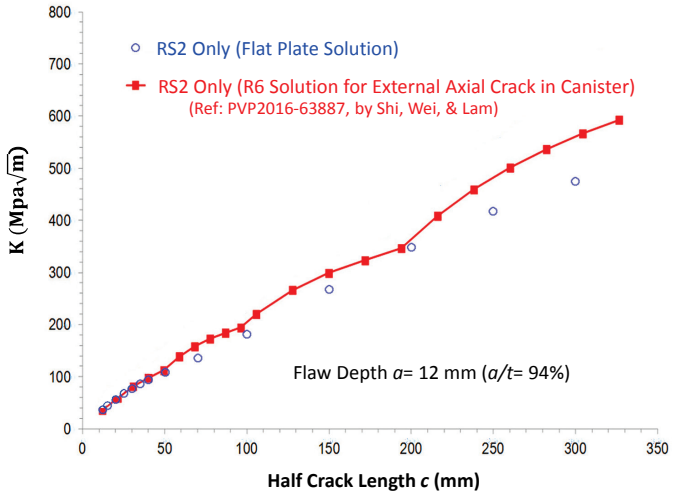

Figure 8 Comparison of Stress Intensity Factor Solutions at the Deepest Point of a Semi-elliptical Crack from R6 for the Canister and from Eq. (2) for an Equivalent Flat Plate

RESULTS AND DISCUSSION

In this section, the stress intensity factors at the surface point (φ= 0, Fig. 9) and at the deepest point (φ= 90°, Fig. 10) of the semi-elliptical cracks are calculated with the flat plate solution, Eq. (2), when the crack is loaded with the bounding WRS defined by Eq. (1). The stress intensity factor is plotted as a function of half crack length (*c*) with various crack depth (*a/t*= 10, 50, 75, and 94%).

Figure 9 indicates that, at the surface point of a shallow (e.g., *a/t* < 50%) semi-elliptical crack, higher stress intensity factor may occur when the crack is short (e.g., *c* < 15 mm). On the other hand, the stress intensity factor at the deepest point of the crack increases with both crack depth and length, as shown in Fig. 10.

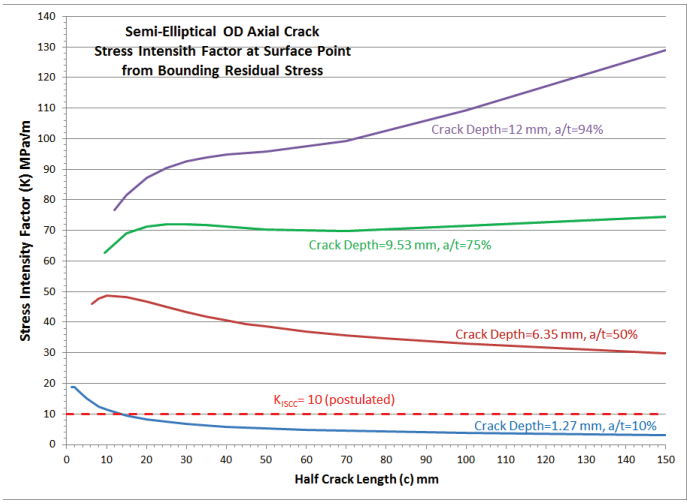

Figure 9 Stress Intensity Factor at the Surface Point (φ= 0°) of an Axial Semi-elliptical Crack under Canister Welding Residual Stress

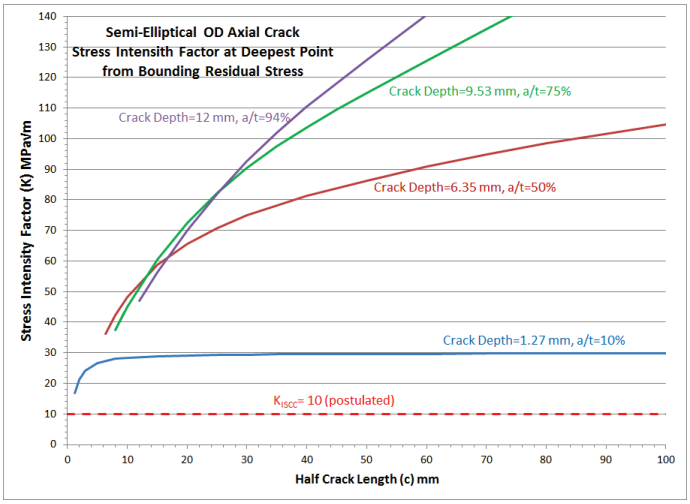

Figure 10 Stress Intensity Factor at the deepest Point (φ= 90°) of an Axial Semi-elliptical Crack under Canister Welding Residual Stress

An important concept for stress corrosion cracking is that, when the stress intensity factor due to loading (including WRS) is greater than the threshold stress intensity factor, K_{ISCC}, stress corrosion cracking may occur. The K_{ISCC} is considered as a material property, dependent on the exposure environment. Many experimental studies have been carried out to determine the K_{ISCC} of 304/304L stainless steels under various exposure conditions. For example, the K_{ISCC} for 304L in 42% $MgCl_2$ solution at 130 °C is about 8 MPa√m and in 22% NaCl solution at 105 °C is 20 MPa√m [14]. However, the experimental investigation of CISCC for stainless steel to determine the crack growth rate (CGR) and the companion K_{ISCC} under an extended storage environment (e.g., in the form of a deposit on

a canister surface as a mixture of moist or deliquesced sea salt and dust) is still in progress [15-17]. Therefore, an arbitrary value of K_{ISCC}= 10 MPa√m is chosen here for demonstration purposes. As seen from Fig. 9, in the case of a shallow surface crack with a/t= 10% (1.27 mm), the stress corrosion cracking will arrest at the surface point when the crack length 2c reaches 28 mm. On the other hand, stress corrosion cracking will occur at the deepest point regardless of the crack length (Fig. 10) for all crack depths considered in this paper. Equivalently, if the K_{ISCC} is greater than 30 MPa√m, and if the sustained external load is relatively small compared to the WRS, then any 10% deep cracks would not be expected to propagate due to stress corrosion cracking.

PATH FORWARD AND CONCLUDING REMARKS

The present stress intensity factor solutions for surface cracks in a canister are based on a flat plate model (Eq. (2)) [11,12]. Although the solution has been validated for a deep crack in Fig. 8, it may be desirable to carry out a comprehensive assessment using a consensus code such as API 579 [5,6] or ASME Section XI [13]. The discrepancies of WRS among various codes and standards and the experimental results may require further research. The critical parameters in stress corrosion cracking, such as K_{ISCC} and the CGR, should also be determined under realistic canister storage conditions. A well-established K_{ISCC} with realistic CGR will be an essential input to the ASME Section XI for the development of Code Case N-860, "Examination Requirements and Acceptance Standards for Spent Nuclear Fuel Storage and Transportation Containment Systems."

The actual stress intensity factor under the influence of WRS would be canister-specific because the welding parameters and materials may be different. A realistic WRS could be obtained by experimental measurement, or more comprehensively by welding simulation using numerical methods for various parameters in canister design. Furthermore, the WRS will be subject to redistribution once a crack is initiated and during subcritical crack growth. In such a case, the ultimate approach is to simulate crack propagation in the WRS field and calculate the stress intensity factors along the crack path as a function of crack length during the quasi-static crack growth. For a growing crack, the difference in the magnitude of stress intensity factor results between the simulation-based and code-based calculations has not been investigated at this time.

The current work is focused on initiation/propagation of "small" flaws due to CISCC. The WRS greatly exceeds the primary stresses in the SNF canister under normal conditions of storage of the canister (i.e., the maximum WRS typically is in the order of magnitude of the yield stress as shown by Figs. 2, 3, 5, and 6). Therefore, the static load of normal storage may be ignored as a driving force for CISCC.

Because of the testing for CISCC initiation (to determine K_{ISCC}) and its subsequent subcritical crack growth (to determine CGR) are sensitive to the stress state of the specimen, the corrosion test design should be selected carefully so the specimen loading represents the nature of the actual stress state as closely as possible. For example, the WRS appears to be in tension through the thickness of the shell (RS2 or RS4 in Figs. 2, 5 and 6). Also, the sections of the canister where CISCC is susceptible are in tension: (1) axial cracks may be subject to tensile hoop stress due to the internal pressure; and (2) circumferential cracks may be under tensile bending stress when this part of canister shell is above the neutral axis with respect to the entire cross-section of the canister, while the other half of the canister is all under compressive bending stress which has no concern for CISCC. In other words, the stress state in the test specimen should be dominated by a tensile stress.

The ASTM E1681 [18] bolt-load compact tension specimen [15,16] would be an appropriate choice because the stress state is mostly tension with a small component of pure bending, which is very similar to the linearized bounding WRS (Eq. (1)) and the cracked plate configuration for calculating stress intensity factor under tension and bending (Eq. (2)). Based on this observation, a surface crack, either formed by machining or by stress corrosion, in the three-point bend or four-point bend specimens [19] may not be suitable for CISCC testing for CGR, especially when the crack has run deep into the thickness of the bend specimen. The general compressive zone below the neutral axis of the test plate under bending will overwhelm the local tensile zone ahead of the small semi-elliptical crack front. This dominating compressive region will limit the capability of the crack to grow under the crack driving force due to CISCC. This would be a mechanical reason to slow down the crack growth as shown by the pure bending specimens [19]. Another possible reason for the slowdown is caused by the depletion of the brine or electrolyte, through which a continuous wetting of the crack is a necessary electrochemical condition for the crack growth to continue. However, that condition may not be sustainable as the crack transcends from a shallow crack to a deep crack in a test with a small droplet of electrolyte applied to the surface of the bend specimen.

ACKNOWLEDGMENTS

This work at the Savannah River National Laboratory was sponsored by the Spent Fuel and Waste and Science Technology (SFWST) Program, Office of Nuclear Energy under the U.S. Department of Energy, and by the Savannah River Nuclear Solutions, LLC under Contract No. DE-AC09-08SR22470 with the U.S. Department of Energy.

The authors wish to express gratitude to Drs. David G. Enos and Charles R. Bryan of the Sandia National Laboratories for providing the welding parameters of the mockup canister and the technical reports. Many important technical bases for ASME Section XI, API 579, and R6 on flaw evaluation procedures have been discussed with Dr. Steven X. Xu of Kinectrics, Inc. (Canada) and with Dr. Liwu Wei of Amec Foster Wheeler (United Kingdom), to whom the authors are indebted for their invaluable assistance.

REFERENCES

[1] Lam, P.S. and Sindelar, R. L "Flaw Stability Considering Residual Stress for Aging Management of Spent Nuclear Fuel Multiple-Purpose Canisters," Journal of Pressure Vessel Technology, 138(4):041406-041406-11, August, 2016, doi:10.1115/1.4032279.

[2] Shi, J., Wei, L. and Lam, P.-S., "Flaw Stability Analysis of Semi-Elliptical Surface Cracks in Canisters under the Influence of Welding Residual Stress," PVP2016-63887, Proceedings of the ASME Pressure Vessels & Piping Conference, Vancouver, BC, Canada, July 2016.

[3] Bjorkman, G., Chuang, T.-J., Einziger, R., Malik, S, Malliakos, A., Mitchell, J, Navarro, C., Ryder, R., Shaukat, S., Ulses, A., and Zigh, G., 2007, A Pilot Probabilistic Risk Assessment of a Dry Cask Storage System at a Nuclear Power Plant, NUREG-1864, U.S. Nuclear Regulatory Commission Washington, DC., USA.

[4] http://www.holtecinternational.com/productsandservices/wasteandfuelmanagement/multi-purpose-canisters/

[5] Fitness-For-Service, API 579-1/ASME FFS-1, June, 2007, American Petroleum Institute, Washington, DC., USA.

[6] Fitness-For-Service, API 579-1/ASME FFS-1, June, 2016, American Petroleum Institute, Washington, DC., USA.

[7] ASME Boiler and Pressure Vessel Code, Section II - Material Specifications, Part D, Properties, American Society of Mechanical Engineers, New York, NY., USA, 2015.

[8] Enos, D.G. and Bryan, C.R., *Final Report: Characterization of Canister Mockup Weld Residual Stresses*, FCRD-UFD-2016-00064, Sandia National Laboratories, November, 2016.

[9] EDF Energy Nuclear Generation Ltd, Assessment of the Integrity of Structures Containing Defects, R6 Revision 4, Including Updates to Amendment 11, December 2014.

[10] BSI, BS 7910:2013+A1:2015: Guide to Methods for Assessing the Acceptability of Flaws in Metallic Structures, December 2013.

[11] Anderson, T.L., *Fracture Mechanics: Fundamentals and Applications*, 2nd Ed., CRC Press, Boca Raton, FL, 1995.

[12] Newman, J.C. and Raju, I.S., "Stress Intensity Equations for Cracks in Three-Dimensional Finite Bodies Subjected to Tension and Bending Loads," NASA Technical Memorandum 86793, NASA Langley Research Center, Hampton, VA, 1984.

[13] ASME Boiler and Pressure Vessel Code, Section XI - Rules for Inservice Inspection of Nuclear Power Plant Components, Nonmandatory Appendix A, Analysis of Flaws, 2015, American Society of Mechanical Engineers, New York, NY., USA.

[14] Cragnolino, G. and Sridhar, N., *A Review of Stress Corrosion Cracking of High-Level Nuclear Waste Container Materials – I*, CNWRA 92-021, Center for Nuclear Waste Regulatory Analyses, San Antonio, TX, August 1992.

[15] Sindelar, R.L., Carter, J.T., Duncan, A.J., Garcia-Diaz, B.L., Lam, P.-S., and Wiersma, B.J. "Chloride-Induced Stress Corrosion Crack Growth under Dry Salt Conditions – Application to Evaluate Growth Rates in Multipurpose Canisters," PVP2016-63884, Proceedings of the ASME Pressure Vessels & Piping Conference, Vancouver, BC, Canada, July 2016.

[16] Duncan, A.J., Lam, P.-S., Sindelar, R.L., and Carter, J.T., "Crack Growth Rate Testing with Instrumented Bolt-Load Compact Tension Specimens under Chloride-Induced Stress Corrosion Cracking Conditions in Spent Nuclear Fuel Canisters," PVP2017-66105, Proceedings of the ASME Pressure Vessels & Piping Conference, Waikoloa, Hawaii, USA, July 2017.

[17] Lam, P.-S. and Kim, Y.-J., *Flaw Stability and Stress Corrosion Cracking of Austenitic Stainless Steel Canisters for Long Term Storage and Transportation of LWR Used Fuel*, Project No. 2016-001-K, U.S.-ROK International Nuclear Energy Research Initiative (INERI), 2016.

[18] ASTM E 1681-03 (2013), "Standard Test Method for Determining Threshold Stress Intensity Factor for Environment-Assisted Cracking of Metallic Materials," ASTM International, West Conshohocken, PA, 2013.

[19] Shirai, K., Tani, J. ,and Saegusa, T., 2011, *Study on Interim Storage of Spent Nuclear Fuel by Concrete Cask for Practical Use - Feasibility Study on Prevention of Chloride Induced Stress Corrosion Cracking for Type 304L Stainless Steel Canister*, CRIEPI N10035, Central Research Institute of Electric Power Industry , Tokyo, Japan (In Japanese).